Electrically Functional Silicone Composites and Their Application in Mechanical Sensors

Chen Guo, Dianming Sun, Chika Takai, Razavi Hadi, Takashi Shirai, Feng Wang, Masayoshi Fuji

Advanced Ceramics Research Center, Nagoya Institute of Technology
3-101-1, Honmachi, Tajimi, Gifu 507-0033, Japan

As a type of special elastomer, silicone elastomer possesses a lot of advantages such as an extreme flexibility, a very wide temperature tolerance range, an excellent insulation and an unparalleled good biocompatibility, which can be utilized in industrial, health care or daily lives. In order to widen the areas of use, overcome some drawbacks of the silicone elastomer, many kinds of functional fillers could be integrated into the elastomer. Just to take advantage of its excellent insulation, inorganic fillers with high dielectric constants, such as $BaTiO_3$ and TiO_2, could be added into the silicone elastomer to fabricate a flexible composite with a high dielectric constant, which can be utilized as an actuator, or be appropriate to be assembled to a tactile or vibration sensor. On the other side, inorganic fillers with high electrical conductivities and large relative surface areas, such as MWCNT, carbon short fiber or graphene, could be integrated into the elastomer to provide a low resistivity. This type of composite has an obvious piezoresistive property, which is suitable for being used within a tactile sensor. Many previous outstanding works were discussed in the article.

Keywords: silicone elastomer; electrical function; barium titanate; dielectric constant; MWCNT; piezoresistive property; mechanical sensor

1. A brief introduction of silicone elastomers

Elastomer is a vague definition of a wide range of polymeric materials. Elastomers are amorphous polymers with glass transition temperatures below room temperature, which display elastomeric behaviors such as viscoelasticity, very weak inter-molecular forces and generally low Young's modulus accompanied with high failure strain compared to other materials. "Rubber" and "elastomer" can be used interchangeably, the latter often refers to synthetically produced elastomeric polymers. An elastomer can be crosslinked or not. A crosslinked elastomer has covalent bonds between the different polymer chains, connecting all of them within a single networked molecule, which prevents the plastic deformation caused by the slippage of molecular chains. An elastomer without chemical covalent bonds usually has physically crosslinks such as hydrogen bonds and Van der Waals forces between their polymer chains, defined as thermoplastic elastomer (TPE) that can be produced with a simple casting molding method and can be recycled. The backbones of the polymer chains in a common elastomer are usually made up of carbon-carbon or carbon-oxygen bonds, the flexibility of the elastomer is related to the saturation levels of the carbon-carbon bonds and the sizes or the cis/trans structures of the side chains.

Silicone, which has a scientific name of polysiloxane, is a series of polymeric materials made up of repeating units of a siloxane with a backbone of alternating silicon atoms and oxygen atoms, frequently combined with side chains of carbon and hydrogen. The chemical structures of the silicone backbones are similar with the structures of quarts, giving it a superb heat-resistant ability [1,2]. A longer bond length and a larger bond angle of silicon-oxygen-silicon bond in silicone lead to an easier configuration variation, which brings a highly flexible behavior. Many benefits are brought from silicone elastomers, such as an excellent environmental resistance, a low compression set, a low level of combustible components, and a high physiological inertness. All types of silicones are known to be good insulation which can act as the substrates of dielectrics [3]. However, there are also some disadvantages of silicone elastomers, such as a poor abrasion, a poor petroleum resistance, and relative low tear strength. Many of them could be overcome by the composite process.

2. Introduction of elastomer-based functional composites

Composites that are made up of functional particles and elastomer have both the functionality of the particles

and the low elastic modules of the elastomer. A poly (dimethylsiloxane)-titania nanocomposites was prepared using heat-treated titania as fillers by Suryakanta Nayak et. al. [4], dielectric and mechanical properties of the composites were measured, it was found that both the dielectric constant and the loss factor of the composites was increased dramatically with the addition of the titanium dioxide filler, whereas resistivity was decreased. Both electrical and mechanical properties were affected by heat treatment of titania particles. It was known that heat treatment decreased the moisture content and also affected the concentration of Ti^{3+} in TiO_2, which in turn affects electrical properties of the system. It was confirmed that presence of surface hydroxyl groups enhances the dielectric constant of the composites. Federico carpi' group [5] firstly reported the embedding of highly dielectric ceramic inclusions in a rubber medium as a method to improve the electromechanical material for dielectric elastomer actuation. In comparison with pure silicone, a decreased elastic modulus, as well as an increased dielectric constant was exhibited. The utilization of this composite as an elastomeric dielectric for planar actuators enabled a reduction of the driving electrical fields. Especially the strain and stress were more than 8 and 4 times higher than the corresponding values that generated with the pure silicone matrix for the analogous electrical stimuli. In Zsolt Varga' study, the magnetic elastomer was prepared by dispersing carbonyl iron particles randomly into dimethylpolysiloxane (PDMS) [6]. It was found that the elastic modulus of this magneto elastomer could be increased by an external magnetic field which is called as temporary reinforcement. Anisotropic samples were prepared by varying the spatial distribution of the magnetic particles in the elastic matrix to enhance the magnetic reinforcement effect. It was found that much larger increase in modulus can be exhibited by the uniaxial field structures than the one with randomly dispersed particles. The most significant temporary reinforcement effect was found if the applied field, the particle alignment, and the mechanical stress are all parallel with each other. A novel polymer composite was developed by Jiawen Xu et al. [7], using self-passivated aluminum particles as the filler. The nanoscale insulating oxide layer of which allows the composites to have a high dielectric constant as a percolation system, while confines the electrons within the aluminum particle, which helps to keep a low loss of the composites. A high dielectric constant with low dissipation factor was obtained from an aluminum/epoxy composite. The thickness of the alumina insulating layer is found to have a negative relation with the particle size. It was found that the polymer matrix can significantly change the dielectric properties of the composites. Functional composites consist of a dielectric active ceramics phase incorporated with a polymer matrix have found use in a variety of applications for sensors and actuators. As the pioneer of this research area, R.E. Newnham has studied a lot of piezoelectric smart composite materials for a wide variety of engineering applications, firstly established the notation for the connectivity of functional composites [8,9]. This notation describes the number of dimensions that each phase is physically in contact with itself. The first number in the notation denotes the physical connectivity of the active phase and the second number refers to that of the passive phase. Composites with 0-3 connectivity consist of functional particles randomly dispersed in a 3D polymer matrix. The primary advantage of a composite with 0-3 connectivity is that it is easy to fabricate, especially to make a thin membrane from it, while remaining the functional activity of the particles [10]. Their research group studied fired 0-3 piezoelectric composites for biomedical ultrasonic imaging applications, consisting of pellets of Lead Zirconate Titanate (PZT) ceramic powders and backfilled with a series of epoxy resins. It was found that composite made out of PZT-Spurr epoxy and fired at 900℃ gave the best performance and the best efficiency as an underwater sensor [11].

3. BT/elastomer composites and their mechanical sensing study

$BaTiO_3$ (which has an abbreviation of BT) is a kind of significant dielectric material with ferroelectric properties under its curie point, which is widely used for ceramic capacitors [12]. The dielectric constant of BT strongly depends on the grain sizes, coarse-grained ceramics of 20~50μm BT show dielectric constant of about 1500~2000 at room temperature, the room-temperature dielectric constant has a maximum of about 3500~4000 when the dense, fine-grained BT has a size of about 1μm [13]. BT with diameters of 300nm and 500nm (BT300 and BT500) that are often utilized in industry were used in the author's previous work. Although having such a high dielectric constant, BT still suffers from some problems such as low breakdown strength, brittleness, and processing difficulties. On the other hand, despite low dielectric constant, organic

polymers have several advantages such as low dielectric loss, high electric breakdown strength, low elastic modules and good processability [14,15]. The problems could be overcome by integrated the BT particles into a flexible elastomer to fabricate a dielectric elastomeric composite, which would lead to a lot of potential novel applications. For instance, a dielectric elastomer actuator can be made by sandwiching membrane of dielectric composites between two compliant electrodes, after loading a voltage between the compliant electrodes, compression in the thickness direction and stretching in area direction of the elastomer membrane could occur due to the Coulombic force [16-21]. On the contrary, a mechanical sensor can be assembled by such a dielectric elastomer and be used to detect the external tactile pressure or mechanical impact by measuring the capacity change.

Because of the poor compatibility between inorganic dielectric particles and organic silicone elastomer, agglomeration of particles is difficult to avoid, bringing a high dielectric loss and a lot of pores that would reduce the dielectric constant of the composite [15]. Consequently, it is of great significance to improve the compatibility between inorganic dielectric particles and elastomers. The reason of improvement of dielectric constant due to the surface modification of the BT particles by the silicone coupling agent is described as below.

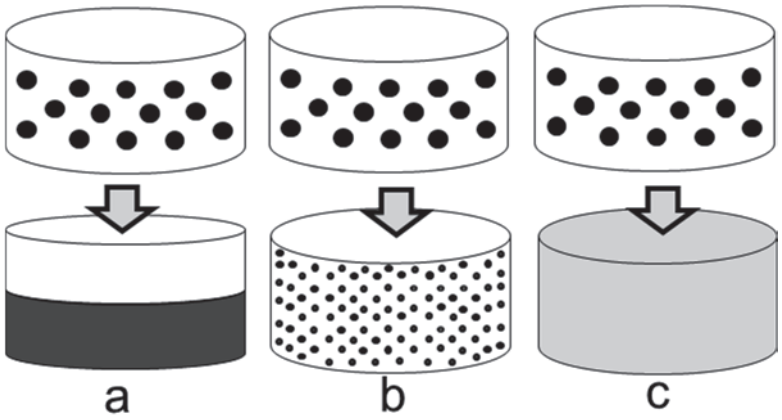

Figure 1 Theoretical models of BT/silicone composites membrane
a: the most serious agglomeration, absolutely divided into two parts
b: the middle status between a and c
c: dispersed very well, absolutely becomes one part

As shown in Fig.1, dispersion status of the BT particles in the silicone elastomer consists of 3 different types. During the fabrication, BT particles are usually dispersed into the uncured silicone elastomer and continually affected by gravity until being cured. The silicone elastomer has a density of 0.93g/cm^3 and the BT particles have a density of about 6.02g/cm^3 which is far more greater than the former, therefore in the curing procedure, the BT particles always tend to precipitate and agglomerate. In Fig.1, part a exhibits an extreme situation that all the BT particles precipitated to the bottom and aggregated, making the whole membrane into two parts: the silicone elastomer part at the upper side and the BT particles part at the bottom. Part c shows an extreme situation oppositely that every single BT particle is separated apart and uniformly distributed in the silicone substrate. Part b is a kind of natural status between situations a and c. As an ideal status, all of the BT particles are distributed into a lot of separated units of agglomeration. Each unit contains several BT particles and is uniformly distributed in the silicone substrate. The size of each unit is not a constant and could vary as the amount of BT particles.

Assume that the dielectric constant of a vacuum is ε_0, the area of membrane is S, the thickness of the membrane is d, and the volume fraction of the BT particles in the composite is x. Every membrane is sandwiched with a good contact by a pair of parallel electrodes with areas of S. Assume that the dielectric constant of the silicone elastomer, BT particles, and the composite is ε_e, ε_f and ε, respectively. The capacitance C of the elastomeric composite can be calculated as follows:

$$C = \frac{\varepsilon_0 \varepsilon S}{d} \qquad (1)$$

For situation a in Fig.1, the capacitance of the silicone

part and the BT part can be calculated, and capacitance of the entire membrane is reversely proportional to the capacitance of the silicone part and the BT part, so the capacitance of the entire membrane can be calculated as:

$$C = \frac{1}{\frac{x}{C_e}+\frac{1-x}{C_f}} = \frac{C_e C_f}{xC_f+(1-x)C_e} = \frac{\frac{\varepsilon_0^2 S^2 \varepsilon_e \varepsilon_f}{d^2}}{\frac{\varepsilon_0 S[x\varepsilon_f+(1-x)\varepsilon_e]}{d}}$$
$$= \frac{\varepsilon_0 S \varepsilon_e \varepsilon_f}{d[x\varepsilon_e+(1-x)\varepsilon_f]} \quad (2)$$

Comparing Eq. (2) with Eq. (1), we can get the dielectric of the membrane as:

$$\varepsilon = \frac{\varepsilon_e \varepsilon_f}{x\varepsilon_e+(1-x)\varepsilon_f} \quad (3)$$

For situation c in Fig.1, the Lenchtenecker' logarithmic law [22] can be used to calculate the dielectric constant of the membrane because of its good dispersity. The dielectric constant of the membrane can be calculated as:

$$\log\varepsilon = (1-x)\log\varepsilon_e + x\log\varepsilon_f \quad (4)$$

From Eq. (4), we can get the dielectric constant:

$$\varepsilon = \varepsilon_e^{(1-x)}\varepsilon_f^x \quad (5)$$

BT particles of 300~500nm have a dielectric constant of about 3300 [23]. According to the previous result, the silicone elastomer has a dielectric constant of about 8. By substituting ε_e=8 and ε_f=3300 into Eq. (3) and Eq. (5), the theoretic dielectric constant of the membrane in situation a and c in Fig.1 can be calculated.

Table1 Theoretical dielectric constant of membrane in situation a and c

volume fraction	10%	20%	30%	40%	50%
ε in situation a	8.9	10.0	11.4	13.3	16.0
ε in situation c	14.6	26.7	48.7	88.9	162.6

As shown in Table1. It is confirmed from the calculated results that within a wide volume fraction range from 10% to 50%, the well dispersed BT/silicone membrane has a higher dielectric constant than the agglomerated one. BT/silicone membranes, in reality, should have a dielectric constant value between situation a and situation c in Fig.1. The dielectric constant of the composite membrane can be raised by improving the dispersity status of the BT particles, making it close to situation c in Fig.1.

Shu-Hui Xie, Bao-Ku Zhu and their coworkers [24] synthesized polyimide/BT composites through a colloidal process, finding that the BT particles in the size of 100 nm were dispersed homogeneously in the polyimide matrix without aggregation. Dang Zhi-Min and his coworkers [25] found that dielectric constant in the polyvinylidene difluoride (PVDF) matrix composites with BT treated by 1.0wt% silane coupling agent KH550 was increased. Their group also found that [26] an appropriate silane coupling agent can be used to improve the interaction between BT and epoxy resin to get a high relative permittivity BT/epoxy resin composites. L. Ramajo et al. [27] studied the influence of silane coupling agents on the microstructure and dielectric behavior of epoxy/BT composites, finding that their composites presented good dielectric properties and a strong dependence on the silane concentration.

In author' previous work [28], to improve the dispersity of BT particles, silicone coupling agent was used to modify their surface. The TG, FTIR results showed that coupling agent was successfully coated on the surface of BT particles. BT/silicone composites membranes were fabricated using raw BT particles and BT particles modified by silicone coupling agent. The particle size distribution measurement and SEM observation showed that BT particles became much more compatible with silicone substrate, the dispersity was considerably improved by surface modification. Dielectric properties were evaluated by LCR meter. The dielectric constant of composites membranes was increased after the dispersion status of BT particles being improved by surface modification with silicone coupling agent. Theoretical calculation from extreme cases proves that agglomeration of BT particles in the vertical direction can seriously reduce the dielectric constant of composites membranes, the dielectric constant can be raised by improving the dispersion of BT particles. Although significantly lower than theoretic values, the piezoelectric properties of BT/Silicone composites show the expectation of being applied in mechanical sensors due to its rapid response to instantaneous electric signals, simple structures, and low costs.

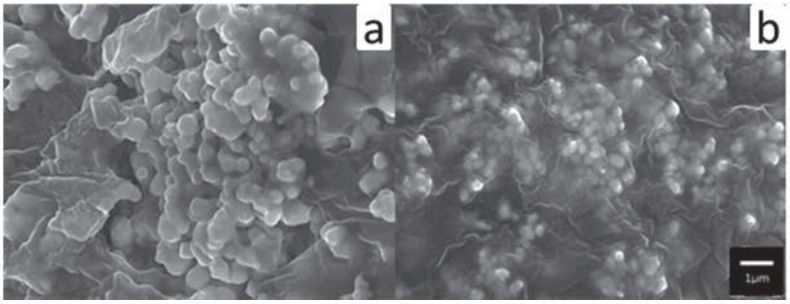

Figure 2 SEM images of cross section of BT/silicone composites
a. raw BT300/silicone composite b. surface modified BT300/silicone composite

Fig.2 shows the SEM images of BT/silicone composites. The cross sections of sample membranes were obtained by breaking them after soaking in liquid nitrogen. Part a shows the SEM image of raw BT300/silicone composites with a volume fraction of 20%. The agglomerates of large amounts of BT300 particles can be clearly observed. At the same time, some cavities can be found in the visual field. To avoid the bubbles as much as possible, mixing of the samples was carried out at vacuum environment. Nevertheless, due to the high viscosity of the BT/silicone mixture, it is almost impossible to eliminating all of the bubbles. Furthermore, due to the large contact angle between BT particles and silicone monomer, it is also impossible to coat the entire surface of the particles and occupy all the space in the composites. BT particles without surface modification are highly hydrophilic while silicone elastomer is highly hydrophobic, during the agglomerating procedure, silicone molecules would be repulsed from around the generated agglomerates and producing many bubbles which would turn into pores after curing. These agglomerates and pores may reduce the dielectric properties of the composites membranes. There is no apparent sign showing silicone has been coated onto the BT particles from the part a, this may due to the poor compatibility between BT and silicone. Part b in Fig.2 shows the SEM image of a sample of 8.57%wt modified BT300/silicone composites with a volume fraction of 20%. It is found that BT particles were dispersed much better than in part a. Although there are still agglomerates in the substrates, their sizes become much smaller and were distributed to a wider area. More importantly, it can be observed that the BT particles are all coated with a layer of silicone elastomer, which may be due to the improved compatibility between BT and silicone after surface modification. Observation of SEM images proves that surface modification by silicone coupling agent can obviously improve their dispersity in silicone elastomer.

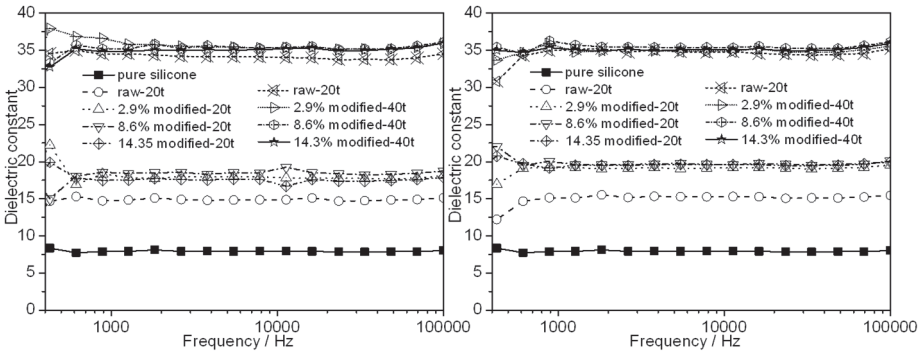

Figure 3 Dielectric constants of BT300/silicone and BT500/silicone membranes at different frequencies

Dielectric properties of BT/silicone membranes were measured by a LCR meter. Dielectric constants of BT300/silicone and BT500/silicone composite membranes with different volume fractions at a frequency from 400Hz to 100kHz are shown in the left side and right side of Fig.3, respectively. It can be known that for every membrane with the same volume fraction but different modification ratios, there is no obvious variation observed from the dielectric constant-frequency curves from low frequency to high frequency.

This is because the whole dielectric properties were measured at a low-frequency area. Obviously, dielectric constant considerably grows as increasing of the volume fraction of BT particles. At a frequency of 10 kHz, the dielectric constant of pure silicone membrane is about 8, and it can be raised to about 35 for raw BT300/silicone membrane with volume fraction of 40%. It is found that the dielectric constant was raised up slightly after surface modification by silicone coupling agent. For example, at a frequency of 10 kHz, for BT300/silicone membrane with a volume fraction of 20%, the dielectric constant changes from 15, 18, 18.5 to 17.5, as modification mass ratio increasing from 0, 2.86%, 8.57% to 14.29%, respectively. And for BT-300/silicone membrane with a volume fraction of 40%, dielectric constants are 34, 34, 35.5 to 35, for membranes with modification mass ratios of 0, 2.86%, 8.57% and 14.29%, respectively. BT-500/silicone membranes show the similar variation and have almost the same dielectric values with the BT-300/silicone membranes. For surface modified BT500/silicone membrane with a volume fraction of 40%, the dielectric constant reaches about 33. There are obvious dielectric loss for the BT/silicone composite due to a lot of factors [14] as follows: Direct current conduct (DC conduct); space charge migration (interfacial polarization contribution); dipole loss caused by movement of molecular dipoles. It is believed that the dielectric loss may decrease after surface modification with silicone coupling agent, because if the majority of BT particles are coated by coupling agent layers with an excellent insulation property, conductivity through BT particles could be significantly reduced, accumulation and migration of electric charge within the composites could be restricted at the same time.

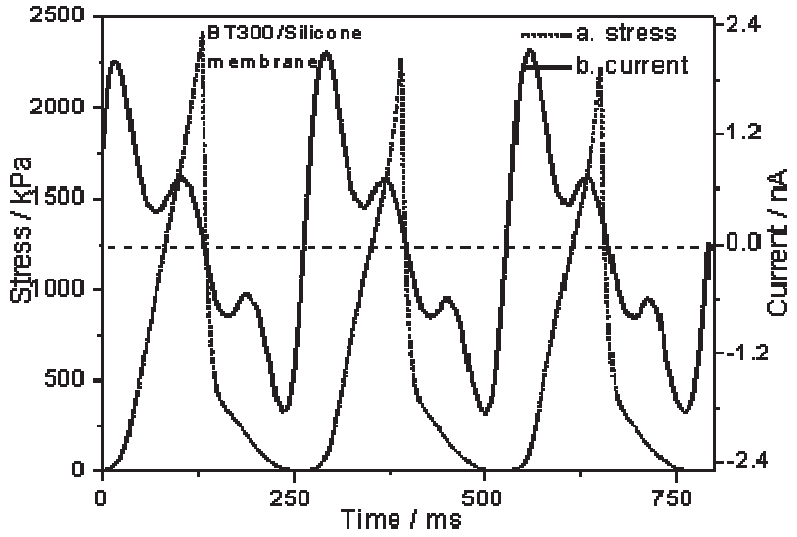

Figure 4 Periodic variation of stress and current of measuring circuit containing BT/silicone membranes

In order to measure the piezoelectricity of the BT/silicone composites, the measuring circuit including a pair of copper electrodes and the composite membranes sandwiched between them was prepared to act as a simple parallel plate capacitor. A multimeter was mounted into the circuit to detect the instantaneous current, a constant voltage of 5V was loaded by a DC power. The membrane accompanied with electrodes was set on a metal plate, a periodical stress was loaded on the membrane by a metal press. Firstly, the press descended with a constant speed of 1000 mm/min, compressing the membrane until its thickness becoming the half; then the press rose up immediately with the same speed until returning to the original position. This procedure was repeated periodically. During the movement, capacitance varies as the changing of thickness, creating a charge-discharge recycle, a weak periodic current could be detected by the multimeter. In the experiment [28], BT300/silicone membrane with a thickness of 3.01mm was used. Fig.4 shows the periodic variation of current occurs in measuring circuit with about 3 cycles. The varying period of current and stress are about 250ms for measuring circuit containing BT300/silicone membrane membrane. For a circuit containing BT300/silicone membrane, stress increases from 0 to about 900kPa and returns to 0 with a sharp peak. It can be found that from cycle 1 to cycle 3, the max stress becomes much smaller, which is due to the stress relaxation of silicone elastomer. At first half period, currents increases from 0 to about 0.9nA

immediately and soon decreases to 0; at the second half period, the currents changes to the opposite direction, like the first half period, then increases from 0 to about 0.8nA immediately and soon decreases to 0. The variation of currents does not show the linear trend mainly because of the nonlinear variation of thickness. The measuring circuit is expected to be appropriate to applications as a mechanical sensor, benefiting from its rapid response to instantaneous electric signals, simple structures, and a low cost.

4. Multi-walled carbon nanotubes/silicone conductive foams and their piezoresistive behaviors

Carbon nanotube (CNT) is a type of cylindrical-like carbon nanomaterial with many unusual properties such as extraordinary thermal conductivity, mechanical and electrical properties which are valuable in many structural and functional applications [29-33]. Especially the multi-walled carbon nanotube (MWCNT) has a relatively low cost and many special behaviors [34-36]. The carbon nanotube has metallic conductivity or semiconducting behavior along its tubular axis. In theory, an armchair type carbon nanotube can carry an electric current density about 1000 times greater than that of copper [37]. Thus CNTs are famous for being investigated as the conductivity enhancing fillers in polymeric composites. J. O. Aguilar et al. studied the influence of CNT clustering on the electrical properties of polymer composite films by comparing the composites with CNTs uniformly dispersed and with those agglomerated in clusters at micro-scale. They found that films with micrometer-size agglomerations have a slightly lower percolation threshold and a higher conductivity than those with uniformly dispersed CNTs, which can be explained that the increased density of CNT-to-CNT junctions favors the formation of the conductive networks [38].

The demand for diverse types of sensors with smart property and low cost is growing rapidly as the recent development of novel technologies, especially artificial intelligence (AI), virtual reality (VR), bionics and biotechnology. Many previous works have been conducted for the implementation of carbon nanotubes in advanced sensor applications [39-45]. M. L. Yola et al. developed a novel imprinted electrochemical biosensor based on Fe@AuNPs and f-MWCNs for direct determination of cefixime (CEF) in human plasma, which showed high sensitivity and selectivity towards CEF and offers the advantages of simplicity and efficiency in target detection from biological samples [39]; their groups also reported the synthesis and application of NiO-multiwall carbon nanotube nanocomposite (NiO/MWCNTs) and 1-butyl-3-methylimidazolium tetrafluoroborate ([Bmim]BF4) in the carbon paste matrix as high sensitive sensors for voltammetric determination of vitamin C in the presence of vitamin B9 in food and drug samples [40]; a robust micro-vibration sensor for biomimetic fingertips was designed by J. A. Fishel et al., which can readily detect the high-frequency vibrations by recording the fluid conducted vibration signals when such a fingertip slides across a ridged surface [41].

MWCNT/polymer conductive nanocomposites have many unique electrical and mechanical properties, such as piezoresistivity, electromagnetic interference (EMI) shielding effect and highly flexibility, which are appropriate for applications as smart functional materials. MWCNT/polymeric conductive nanocomposites provide obvious piezoresistive behaviors, having applications in many special fields due to their high flexibility, which can be easily produced with large sizes and very low costs. The strain-dependent electrical resistance characteristics of MWCNT/polyethylene oxide (PEO) were investigated in the research of Park, M. et al. Unique and repeatable relationships in resistance versus strain were obtained, the overall pattern of which was found consists of linear and nonlinear regions. This type of material was expected to be used as tunable strain sensors such as sensors embedded into systems [46]. Al-Saleh et al. analyzed the EMI shielding mechanisms of MWCNT/polypropylene composite plates experimentally and theoretically, found that the absorption is the major shielding mechanism and the reflection is the secondary shielding mechanism. A negative influence on the overall EMI shielding effectiveness brought by multiple-reflection was shown by the theoretical analysis. They believed that a multi-surface shield such as conductive polymer composites might drastically enhance the overall EMI shielding effectiveness if multiple-reflection can be minimized [47].

Elastomer, such as a silicone elastomer, is a type of material with high flexibility, which acts as an excellent matrix for tactile sensors or actuators [48]. However, it also has some disadvantages, like low tear strength, a relatively high density, and an obvious viscoelasticity. Foaming is a method to overcome this disadvantage [49-

53]. The flexibility can be significantly improved by the foaming procedure. The viscoelasticity can be reduced drastically as a shift of the deforming configuration. K. A. Klicker et al. explored the effect of porosity on the hydrostatic piezoelectric sensitivity of 3-1 connectivity in a foamed polyurethane matrix [52]. They found that the piezoelectric coefficient under hydrostatic loading sharply increases when porosity is incorporated to 40%. As an important method to enhance the sensitivity of the piezoresistive property, foaming process has been widely used to the conductive nanocomposites in industry. The piezoresistive properties of MWCNT/polymer unfoamed composites have been reported by many previous works. However, there is almost no report about the piezoresistive properties of foamed MWCNT/polymer composites from other research groups. In author's study [54], a series of novel MWCNT/silicone conductive foamed nanocomposites were fabricated. The diverse porous structures, the distribution-orientation status of the MWCNTs in the silicone matrix were observed by a laser microscope and SEM with or without a compressive load. The influences of the porous structure and porosity on the foam density, elastic modulus, resistivity as well as piezoresistive property were studied. A piezoresistive model for the foamed conductive fillers reinforced elastomeric composites was developed, the calculated results of the resistive variations were used to compare to the measured values.

Various theoretical electrically conductive models and piezoresistive models have been developed in many previous works [55-57]. In M. Taya' work, an analytical modeling was developed to study the piezoresistive behavior of a conductive short fiber reinforced elastomer composite, the reorientation distributions of the conductive short fibers due to stretching strain were computed by using a fiber reorientation model. It was found that the threshold fiber volume fraction increases as the applied strain increases [58]. An analytical model of the effective electrical conductivity of carbon nanotube composites was developed by Fei Deng et al., which takes account of not only the CNT concentration and percolation, but also CNT conductivity anisotropy, aspect ratio and non-straightness [59].

In the works of Xiang-wu Zhang [60,61], the total resistance in conductive composites is considered to be a function of both the resistance through each conducting particle and the polymer matrix. The resistivity of the matrix is assumed to be constant everywhere, the resistance of the conductive paths perpendicular to the current flow was neglected. Then the number of the conductive particles between electrodes, the number of the conducting paths and the average distance between the adjacent particles become the main factors, the resistance for the conductive composites can be described as

$$R = \frac{M}{N}\left[\frac{8\pi hs}{3A\gamma e^2}\exp(\gamma s)\right] \qquad (6)$$

where

$$\gamma = \frac{4\pi}{h}\sqrt{2m\varphi} \qquad (7)$$

s is the average minimum distance between two adjacent conductive particles, A is the effective cross-sectional area of one electrically conducting path, h is Plank' constant, e and m are the electron charge and electron mass, φ is the tunneling potential barrier height, N is the number of conducting paths in the composite and M is the number of conductive particles forming one conducting path. If the initial average minimum distance between two adjacent conductive particles and the initial resistance is assumed as s_0 and R_0, respectively, the relative resistance of the conductive composites when a stress is applied can be described as

$$\frac{R}{R_0} = \frac{s}{s_0}\exp[\gamma(s - s_0)] \qquad (8)$$

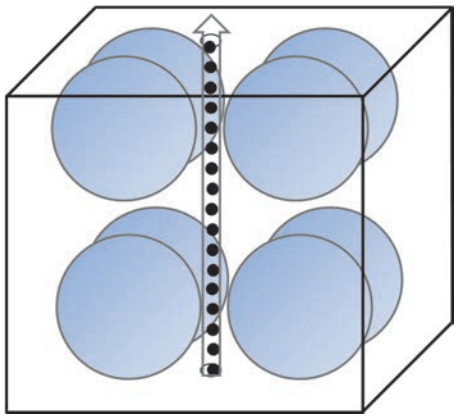

Figure 5 An image of an electrically conductive path in a cubic space of the conductive foamed composite

Considering the situation of the conductive foamed composite, the compression would become much more complex because of the influence of the porous structure on the elastic modulus. A cubic space in the conductive foam with a length of L was illustrated in the Fig.5. Both voids and conductive particles were assumed as spherical shapes and to be distributed in the polymer matrix with absolute homogeneities. The voltage was loaded to the composite, making the current flow

through the vertical direction. The current was thought homogeneously distributed in the space without being blocked by the voids through the vertical direction. One of the conducting paths was shown in the Fig.5, which was thought to keep being perpendicular to the horizontal plane. If a uniaxial pressure is loaded on the conductive foam through the vertical direction, the cubic space will be compressed, the average distance between the conductive particles will be shortened and the resistance of the conductive foam through the vertical direction will be reduced. However, the influence of the voids on the compressing procedure is extremely complex, making it difficult to calculate the piezoresistive property of the conductive foam.

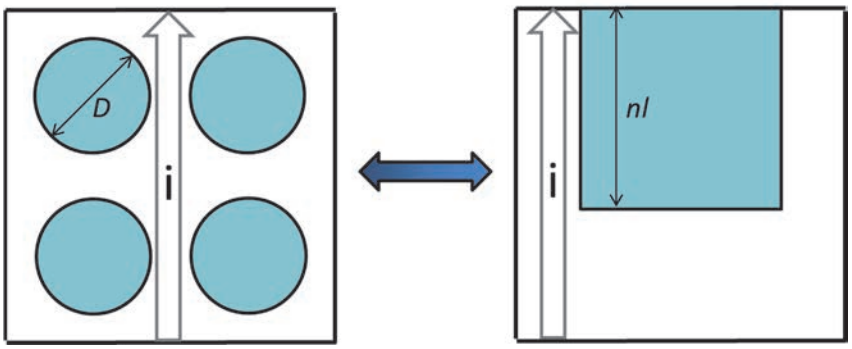

Figure 6 The flow chart of simplification of the piezoresistance analysis of a cubic space in the conductive foamed composite

In order to simplify the calculation procedures, several assumptions were made for the voids: The spherical voids with an average diameter D were treated as cubic shapes with an average length of l and could maintain a constant average volume. As shown in the Fig.6, the vertical plane from the Fig.6 was illustrated. One electrically conductive path through the vertical direction was shown in the Fig.6. Therefore

$$\frac{\pi}{6}D^3 = l^3 \qquad (9)$$

$$l = \left(\frac{\pi}{6}\right)^{1/3} D \qquad (10)$$

the effect of the pressure of confined gas in the voids and the atmospheric pressure on the compressing procedure was neglected; the number of conductive particles within one conductive path in the cubic space was expressed as n. These cubic-like voids in this cubic space were assumed to be combined together as a big cubic-like void, which has a length of nl. This big void was thought to be able to move freely within the cubic space without affecting the calculation of the piezoresistive property due to its cubic shape. Assume that it was moved to the top of the cubic space, dividing the space into a "hollow" part at the top and a "solid" part inferior. The length of the big cubic-like void is

$$nl = \sqrt[3]{\frac{(1-\rho_r)L^3}{l^3}} \cdot l = (1-\rho_r)^{\frac{1}{3}} \cdot L = kL \qquad (11)$$

Thus the ratio of the length of the big cubic void versus the length of the entire cubic space can be calculated as

$$k = \frac{nl}{L} = (1-\rho_r)^{1/3} \qquad (12)$$

Here ρ_r is the relative density of the conductive foam (the density of the conductive foam divided by the density of the unfoamed conductive composites with the same volume fraction of conductive particles). l is the length of a single void before combination, L is the length of the big void after combination, respectively.

When an external force was loaded on the cubic space though the vertical direction, the compressive strain of the upper "hollow" part ε_h and the compressive strain of the inferior "solid" part ε_s were different because of the different force areas. Considering this difference and neglecting the compression of the conductive particles, the average inter-particle distance s in the conductive foam can be calculated as

$$s = s_0[1-\varepsilon_h-\varepsilon_s] = s_0\left[1-\left(1-k+\frac{k}{1-k^2}\right)\frac{\sigma}{E}\right] \qquad (13)$$

In which σ is the applied uniaxial stress, E is the elastic modulus of the unfoamed conductive composites with the same volume fraction of conductive particles. The average inter-particle distance can be calculated as

$$s_0 = d\left[\left(\frac{\pi}{6}\right)^{1/3}\left(\frac{f}{\rho_r}\right)^{-1/3} - 1\right] \qquad (14)$$

In which d is the average particle diameter, f is the volume fraction of the conductive particle in the conductive foam, f/ρ_r is thought as the "real" volume fraction in the polymer matrix. Then substitute the Eq. (13) and Eq. (14) into the Eq. (8), the relative resistance

of the conductive foam when a stress is applied can be calculated as

$$\frac{R}{R_0} = \left[1 - \left(1 - k + \frac{k}{1-k^2}\right)\frac{\sigma}{E}\right] \exp$$

$$\left[-\frac{\sigma\gamma s_0}{E}\left(1 - k + \frac{k}{1-k^2}\right)\right] \quad (15)$$

The piezoresistive property can be simply estimated with the Eq. (15). This piezoresistive model can be used to predict the effect of the porosity of the conductive foam on its piezoresistance effectively. However there are some drawbacks in this model which would reduce the accuracy of the prediction: Pores in the conductive foam were considered as cubic shapes, which have a different compression mode with the spherical one. Furthermore, the average pore diameter was neglected due to the combination of the pores; the competition between the pressures of the gas confined in the pores and the atmospheric pressure was neglected, which in fact brings some effect on the compressing procedures; the electrically conductive particles were assumed to be spherical. In fact, many fiber-like or sheet-like conductive particles were found to have lower percolation thresholds and be much more effective in conductivity enhancing compared to the spherical particles.

In author' previous work [62], piezoresistive models for fiber-like conductive fillers/polymeric solid composites and for fiber-like fillers/polymeric foam were both developed. Those models were designed to reflect the effects of both the displacement and orientation of the fiber-like fillers precisely, although leading to some extremely complex calculation and thereby reduce the practicability. The Eq. (15) accompanied with Eq. (12) and Eq. (14) was used to calculate the piezoresistive variations of the MWCNT/silicone conductive foams and the results were used to compare to the measured values.

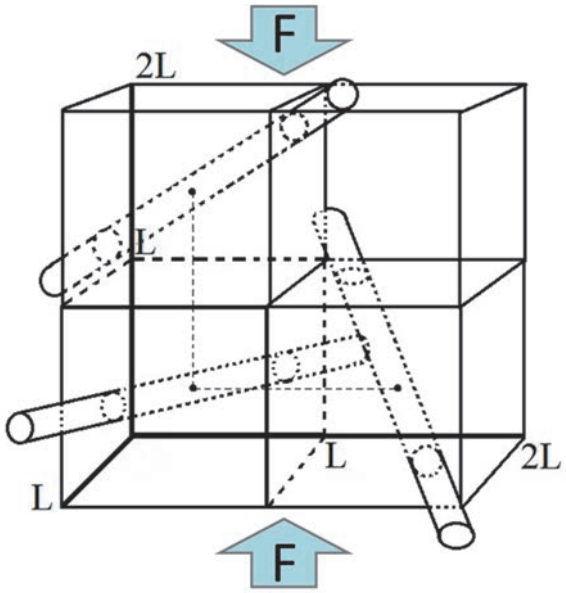

Figure 7 A brief image of the compressing procedure of unfoamed MWCNT/silicone elastomers by external pressure

Many types of fiber-like carbon fillers such as carbon nanofiber (CNT) are found useful to confer conductivity and piezoresistivity [63-66]. There are more opportunities for the formation of the conductive paths in the fiber-like particles filled composites. The distributions and orientations of the fiber-like fillers always change with the deformation of the substrates, leading to a unique alteration of conductivity. Many previous works focused on the piezoresistivity brought by fiber-like particles [67-70].

According to the Eq. (8), if a pressure is loaded on the composite, the average minimum distance between adjacent MWCNTs will be changed from s_0 to s_1, the resistance will become from R_0 to

$$R_1 = \frac{s_1 A_0 R_0}{s_0 A_1} \exp\left[\frac{4\pi}{h}\sqrt{2m\varphi}(s_1 - s_0)\right] \quad (16)$$

As shown in Fig.7, the MWCNTs dispersed in the substrates are described as ideal cylinders with the same length and the same radius of l and r. The continuous substrate is described as divided cube-like rooms which all have a same edge length of L, so the average minimum distance between adjacent MWCNTs s ranges randomly from 0 to L. The MWCNTs are thought to be distributed in the substrate absolutely homogeneously,

whose centers absolutely coincide with the centers of the cubes. When the composite deforms under the uniaxial pressure from the vertical direction, the edge length L is assumed to vary with the deformation. θ is the angle between the shortest connecting line of two adjacent fibers and the uniaxial pressure direction, which ranges from 0 to π randomly. ε is the compressing strain of the composite, so

$$\frac{s_1}{s_0} = 1 - \varepsilon(\cos^2\theta - \upsilon\sin^2\theta) \qquad (17)$$

Substitute it into the Eq. (8), the resistance of the composite under a pressure can be randomly calculated as

$$R_1 = \frac{A_0 R_0}{A_1}[1 - \varepsilon(\cos^2\theta - \upsilon\sin^2\theta)]\exp$$

$$\left[\frac{4\pi\varepsilon s_0}{h}\sqrt{2m\varphi}(\upsilon\sin^2\theta - \cos^2\theta)\right] \approx R_0\exp$$

$$\left[\frac{4\pi\varepsilon s_0}{h}\sqrt{2m\varphi}(\upsilon\sin^2\theta - \cos^2\theta)\right] \qquad (18)$$

If the relationship between θ and s is neglected, the average resistance of composite under a pressure can be calculated by

$$\overline{R_1} \approx \frac{R_0}{\pi L}\int_0^{\pi}\int_0^{L}\exp\left[\frac{4\pi\varepsilon s_0}{h}\right.$$

$$\left.\sqrt{2m\varphi}(\upsilon\sin^2\theta - \cos^2\theta)\right] ds_0 d\theta$$

$$= \frac{R_0}{\pi L}\int_0^{\pi}\left\{\frac{h\exp\left[\frac{4\pi\varepsilon L}{h}\sqrt{2m\varphi}(\upsilon\sin^2\theta - \cos^2\theta)\right] - h}{4\pi\varepsilon\sqrt{2m\varphi}(\upsilon\sin^2\theta - \cos^2\theta)}\right\} d\theta \qquad (19)$$

The effective volume fraction of MWCNTs can be thought as

$$f = \frac{\pi l^3}{48L^3} \qquad (20)$$

Therefore the average resistance of composite under pressure can be described as

$$\overline{R_1} \approx R_0\left(\frac{48f}{\pi^4 l^3}\right)^{\frac{1}{3}}\int_0^{\pi}$$

$$\left\{\frac{h\exp\left[\frac{4\varepsilon}{h}\left(\frac{\pi^4 l^3}{48f}\right)^{\frac{1}{3}}\sqrt{2m\varphi}(\upsilon\sin^2\theta - \cos^2\theta)\right] - h}{4\pi\varepsilon\sqrt{2m\varphi}(\upsilon\sin^2\theta - \cos^2\theta)}\right\} d\theta \qquad (21)$$

In author's previous work [62], novel highly sensitive piezoresistive foams with excellent elasticity were fabricated by adding a new type of thermally expandable microbeads, which leads to a cell-filled flexible structure. Effects of MWCNT and the foaming agent on the piezoresistivity were investigated. The deformation of the cross section caused by a uniaxial pressure was observed originally and its effect on the piezoresistivity was discussed in detail.

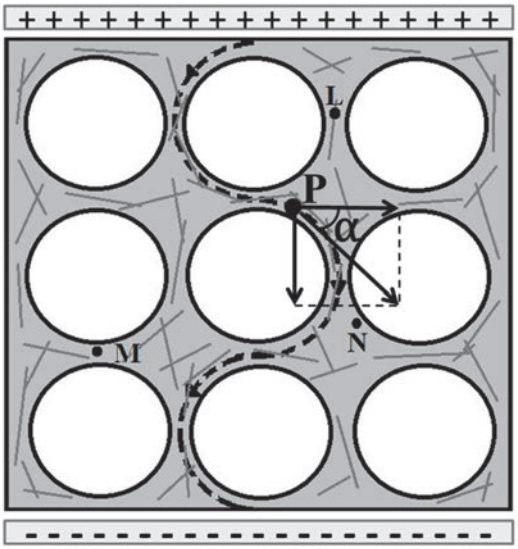

Figure 8 A brief image of the piezoresistive mechanism for microbeads cells filled conductive composites

The mechanism for the microbeads loaded MWCNT/ silicone elastomeric composite was also discussed. As it shows in the Fig.8, the electric conductive paths are confined in the matrix area between the insulated cells. According to the SEM observation result, the cells were slightly being compressed when the foams were under a uniaxial pressure. In order to simplify the piezoresistive model, some assumptions are made: The cells always keep perfect sphere-like shapes when under a pressure; the current passes through the foam matrix along the edges of these cells; the Poisson's deformation of the substrate area with cells only in its horizontal direction, such as the point L in the Fig.8, would be absolutely blocked by the adjacent cells; the Poisson's deformation would not be affected in the substrate area with cells only in its vertical direction, like the point M; the Poisson's deformation of the other areas, such like the point N, would be partially affected. Based on these assumptions, the Eq. (6) and Eq. (8) can be used to describe the piezoresistive phenomenon of the cell introduced foams, in which the conductive paths become to longer semicircle. As in the Fig.8, for the point P in the conductive path from A to B, if the angle between the conductive direction and the horizontal direction is set as α, the ratio of the average minimum distance between adjacent MWCNTs in the foam before and after compression will be

$$\frac{s_1}{s_0} = 1 - \int_0^{\pi}\varepsilon(\cos^2\theta\cdot\sin\alpha - \upsilon\sin^2\theta\cdot\cos a)\,d\alpha$$

$$= 1 - 2\varepsilon\cos^2\theta \qquad (22)$$

Substitute it into the Eq. (8), use the same method in Eq.

(17) ~ Eq. (21), the average resistance of the foam under a pressure can be easily calculated as

$$\overline{R_1} = R_0\left(\frac{48f}{\pi^4 l^3}\right)^{\frac{1}{3}} \int_0^{\pi} \left\{ (1 - 2\varepsilon\cos^2\theta) \cdot \frac{h\exp\left[\frac{4\varepsilon}{h}\left(\frac{\pi^4 l^3}{48f}\right)^{\frac{1}{3}}\sqrt{2m\varphi}(\upsilon\sin^2\theta - \cos^2\theta)\right] - h}{4\pi\varepsilon\sqrt{2m\varphi}(\upsilon\sin^2\theta - \cos^2\theta)} \right\} d\theta \qquad (23)$$

The theoretical values calculated by Eq. (21) and Eq. (23) were used to compare with the experimental results, relatively well-fit results were obtained.

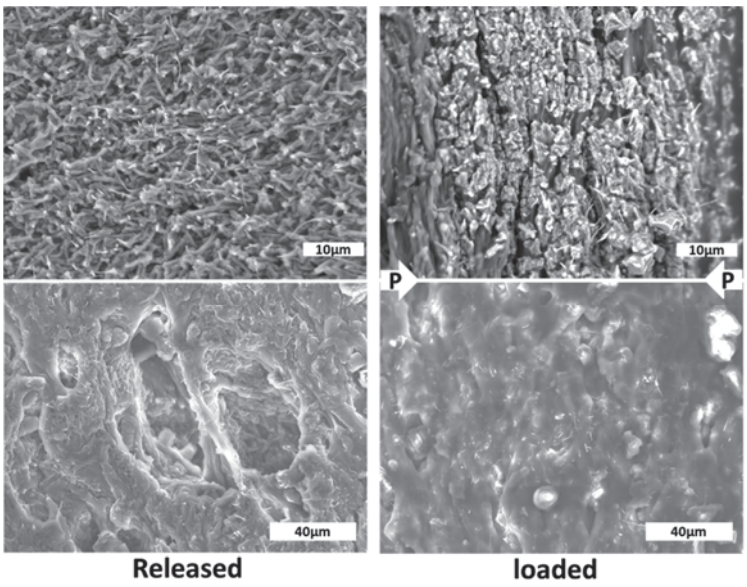

Figure 9 SEM images of the MWCNT/silicone conductive composite foamed by ADCA under and without a uniaxial load

In author' previous work [54], the MWCNT/silicone elastomeric composites were fabricated and foamed by 3 different types of foaming agents. The backscattered electron images of the dispersed MWCNT particles were taken at a high magnification while normal SEM images of the voids structures were taken with a low magnification. The images of the MWCNT/silicone conductive elastomeric composite foamed by azodicarbonamide (ADCA) without a compression strain were shown at the left hand of Fig.9. Large amounts of MWCNT particles were found to be distributed homogeneously in the silicone matrix. The majority of which were found being covered tightly with silicone elastomer except for several half-naked particles distributed in the cross-section surface. These covered MWCNT particles contacted, overlapped each other and formed cluster-liked conductive networks. It is believed that the coated silicone layers interrupted the direct contact between the MWCNT fibers, making the resistivity of the conductive foams become much more changeable. It can be found that all the MWCNT fibers were distributed in the silicone matrix with random orientations before compression. The images of the MWCNT/silicone elastomeric composite foamed by ADCA under a compression strain of 75% were shown at the right hand of Fig.9, the majority of the MWCNT fibers were found to orient to the direction perpendicular to the compressive strain, the contact and overlapping were found dramatically enhanced by the external pressures. This is considered to be the main enhancement factor of the piezoresistive phenomenon of the MWCNT/silicone elastomeric composites.

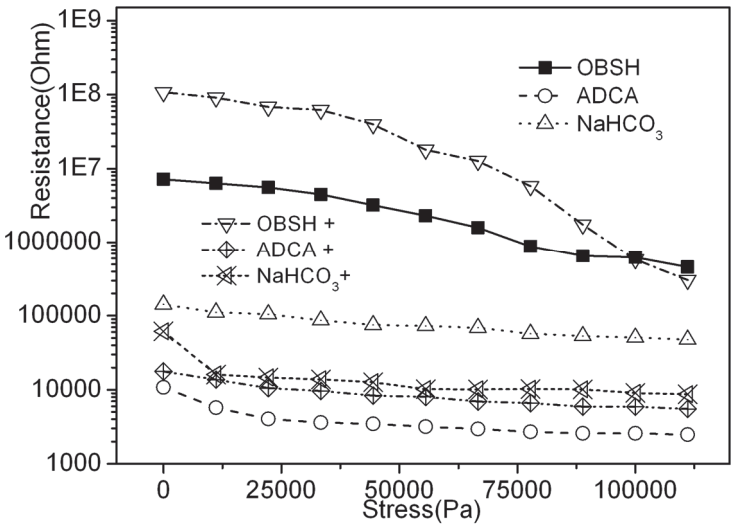

Figure 10 Piezoresistive properties of the MWCNT/silicone conductive foams

The piezoresistive properties of the MWCNT/silicone elastomeric conductive composites with all types of foaming agents, including p,p'-oxybis(benzenesulfonylhydrazide) (OBSH), azodicarbonamide (ADCA) and sodium hydro carbonate foaming agents ($NaHCO_3$), were shown in Fig.10, illustrating the resistance-stress connections. The resistance decrease can be found from all samples as the increase of the stress, almost all of the resistance-stress curves were found to be nonlinear, due to their complex foam compression modes. Obvious decreases can only be found from the OBSH foamed samples, especially from the one with a higher foaming ratio. This demonstrates that a lower elastic modulus brought by a foaming agent with a high foaming efficiency leads to a higher piezoresistive sensitivity, which can be enhanced simply by increasing the loading of the foaming agent. The resistances of the OBSH foamed samples dropped obviously when loaded with a uniaxial stress of about 110kPa. It is believed that the voids in the foams occupied much space of the silicone matrix, enlarged the distances between the MWCNT particles. Therefore the resistivity was improved significantly. The resistance changes are precise and rapid enough to be utilized within a piezoresistive tactile sensor. Oppositely, only slight resistance decreases were obtained from ACDA and the $NaHCO_3$ samples due to the relative lower foaming efficiencies of the ACDA and the $NaHCO_3$ foaming agents. It is also noteworthy that the resistances maintained in higher ranges for OBSH foamed samples and in lower ranges for other samples. An obvious increase of the whole resistance range was brought to the silicone matrix by the OBSH foaming agent.

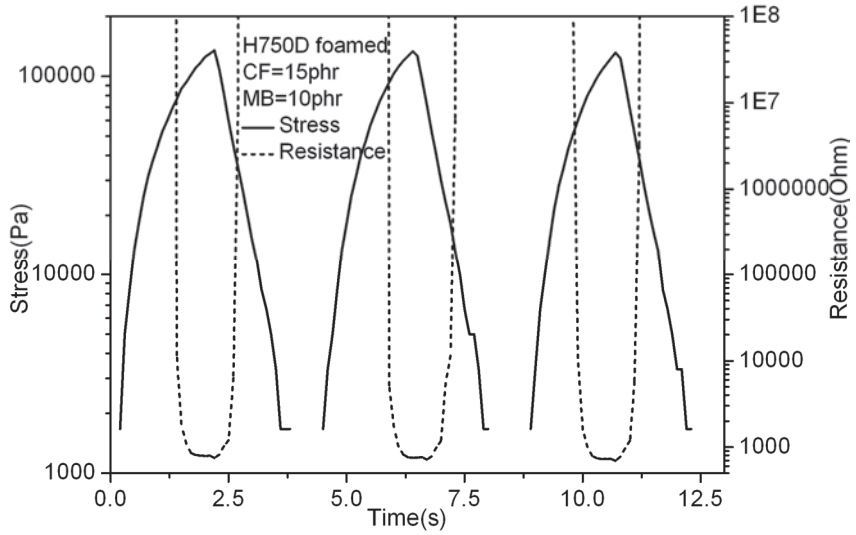

Figure 11 Piezoresistivity of the MWCNT/silicone composite foamed by H750D microbeads under periodic pressures

In author' another work [62], the MWCNT/silicone elastomeric conductive composites foamed by thermal expand microbeads were fabricated. The piezoresistivity of the MWCNT/silicone composite foamed by H750D microbeads under periodic pressures are shown in the Fig.11. The measurements for the composite with an MWCNT content of 15phr and with a H750D microbeads content of 10phr are shown in Fig.11. Compared to the unfoamed elastomer, the piezoresistivity curve of the composite shows a much shorter period. The peaks of the curve are synchronous well with the peaks in the stress curve. An obvious and rapid recovering of the resistances can be clearly observed because the introduction of the foaming agents changed the compression mode of the composites. H750D foaming agent is microbeads which can keep their stiffness in some degree even after expanding. The existence of the microbeads cells drastically reduces the viscous flow of the silicone molecule chains. It is convinced that addition of the microbeads foaming agents can effectively improve the sensitiveness and repeatability of the MWCNT/silicone composites.

5. Conclusion

Silicone elastomer has a lot of advantages being used as the substrate of the electrically functional elastomeric composite. Taking advantage of excellent insulation of silicone elastomer, inorganic fillers with high dielectric constants, such as BT and TiO_2, could be added into the silicone elastomer to fabricate a flexible composite with a high dielectric constant, which can be utilized as an actuator or be assembled to a mechanical sensor. In author' study, BT/silicone membranes were fabricated using raw BT particles and BT particles modified by novel silicone coupling agent. It was found that the dispersity of BT particles in silicone substrate was considerably improved after surface modification. Dielectric properties were evaluated by an LCR meter, the results showed that dielectric constants of composites membranes were increased after improving the dispersion status of BT particles. Theoretical calculation from extreme cases proves that agglomeration of BT particles in vertical direction could seriously reduce the dielectric constants of composites membranes, the dielectric constant could be raised by improving the dispersion of BT particles. The current generated by variation of BT/silicone membrane was detected, which is expected to be applied to mechanical sensors applications due to its rapid response to instantaneous electric signals, simple structures, and low costs.

On the other side, electrically conductive particles with large relative surface areas such as MWCNT, carbon short fiber or graphene, could be integrated into the elastomer to provide a low resistivity. This type of composite has an obvious piezoresistive property, which is suitable for application in a mechanical sensor. In author' previous works, novel MWCNT/silicone conductive foamed nanocomposites were fabricated with an OBSH, an ADCA and a $NaHCO_3$ type foaming agents. The porous structures of the foamed composites, the distribution-orientation status of the MWCNTs in the silicone matrix were both observed with a laser microscope and a SEM. It was found that the majority of the voids in the matrix was being crashed by the external pressure, which leads to a reduced modulus and improves the piezoresistive property of the composites. The contact and overlapping of the MWCNT particles were found dramatically enhanced by the pressure-caused reorientation, which is considered to be the main enhancing factor of the piezoresistive phenomenon of the MWCNT/silicone conductive composites. The densest and finest porous structures were obtained by using the OBSH foaming agent which has the best affinity with the silicone elastomer and a highest foaming efficiency. The most sensitive piezoresistive property was obtained by the OBSH foamed MWCNT/silicone conductive nanocomposite. Another type of novel highly sensitive piezoresistive composites was fabricated using MWCNT, silicone elastomer, and thermal expanding microbeads foaming agent. It is found that the confinement of MWCNT particles by microbeads cells improves the piezoresistive sensitiveness and repeatability. Well fit were found between the theoretical calculations and the experimental piezoresistivity measurements of these MWCNT/silicone elastomeric composites. In the future work, mechanical sensors will be assembled with the BT/silicone elastomeric composites or MWCNT/silicone elastomeric composites to detect static pressures and impacts.

REFERENCES

[1] S. Nayak, M. Rahaman, a. K. Pandey, D.K. Setua, T.K. Chaki, D. Khastgir. J. Appl. Polym. Sci. 127, 784–796 (2013).

[2] J.W. Liou, B.S. Chiou. Electron. Eng. 10, 2773–2786 (1998).

[3] E. a. Cherney. Annu. Rep. - Conf. Electr. Insul. Dielectr.

Phenomena, CEIDP. 1–9 (2005).

[4] Nayak, S., Rahaman, M., Pandey, A. K., Setua, D. K., Chaki, T. K., & Khastgir, D. Journal of Applied Polymer Science, 127(1), 784-796 (2013).

[5] Carpi, F., & Rossi, D. D. IEEE Transactions on Dielectrics and Electrical Insulation, 12(4), 835-843 (2005).

[6] Varga, Z., Filipcsei, G., & Zrínyi, M. Polymer, 47(1), 227-233 (2006).

[7] Xu, J., & Wong, C. P. (2004). In Advanced Packaging Materials: Processes, Properties, and Interfaces, 2004. Proceedings, 9th International Symposium on (pp. 158-170). IEEE.

[8] Newnham, R. E., D. P. Skinner, and L. E. Cross. Materials Research Bulletin, 13(5), 525-536 (1978).

[9] Newnham, R. E., and Gregory R. Ruschau. Journal of Intelligent Material Systems and Structures 4(3) 289-294 (1993).

[10] Tressler, J. F., S. Alkoy, A. Dogan, and R. E. Newnham. Composites Part A: Applied Science and Manufacturing 30(4) 477-482 (1999).

[11] Madhavan, C., T. R. Gururaja, T. T. Srinivasan, Q. C. Xu, and R. E. Newnham. In IEEE 1987 Ultrasonics Symposium, 1987 (pp. 645-650). IEEE.

[12] D. Hennings, G. Rosenstein. J. Am. Ceram. Soc. 67249–254 (1984).

[13] G. Arlt, D. Hennings, G. De With. J. Appl. Phys. 58, 1619–1625 (1985).

[14] K. Yang, X. Huang, Y. Huang. Chem. 25, 2327–2338 (2013).

[15] L. Xie, X. Huang, Y. Huang, K. Yang, P. Jiang. J. Phys. Chem. C. 117 (2013).

[16] Y. Liu, L. Liu, Z. Zhang, J. Leng. Smart Mater. Struct. 18, 095024 (2009).

[17] F. Carpi, D.D. Rossi. Dielectr. Electr. Insul. IEEE Trans. 12, 835–843 (2005).

[18] F. Carpi, G. Gallone, F. Galantini, D. De Rossi. Adv. Funct. Mater. 18, 235–241 (2008).

[19] B. Kussmaul, S. Risse, G. Kofod, R. Waché, M. Wegener, D.N. McCarthy, et al. Adv. Funct. Mater. 21, 4589–4594 (2011).

[20] A. O'Halloran, F. O'Malley, P. McHugh. J. Appl. Phys. 104, 1–10 (2008).

[21] P. Brochu, Q. Pei. Macromol. Rapid Commun. 31, 10–36 (2010).

[22] R. Sengupta, S. Chakraborty, S. Bandyopadhyay, S. Dasgupta, R. Mukhopadhyay, K. Auddy, et al. Engineering. 47, 21–25(2007).

[23] S. Wada, H. Yasuno, T. Hoshina, S.-M. Nam, H. Kakemoto, T. Tsurumi. J. Appl. Phys. 42, 6188–6195 (2003).

[24] Shu-Hui Xie, Bao-Ku Zhu, Xiu-Zhen Wei, Zhi-Kang Xu, You-Yi Xu. Composites Part A: Applied Science and Manufacturing. 36, 1152-1157 (2005).

[25] Dang, Zhi-Min, Wang Hai-Yan, Xu Hai-Ping.Applied Physics Letters. 89, 112902 (2006).

[26] Zhi-min Dang, Yan-Fei Yu, Hai-Ping Xu, Jinbo Bai. Composites Science and Technology. 68, 171-177 (2008).

[27] L. Ramajo, M.S. Castro, M.M. Reboredo. Composites Part A: Applied Science and Manufacturing. 38, 1852-1859 (2007).

[28] Guo, C., & Fuji, M. Advanced Powder Technology, 27(4), 1162-1172 (2016).

[29] R. George, K.T. Kashyap, R. Rahul, S. Yamdagni. Scr. Mater. 53, 1159-1163 (2005).

[30] J.A. Kim, G.S. Dong, T.J. Kang, J.R. Youn. Carbon. 44, 1898-1905 (2006).

[31] W.A. Curtin, B.W. Sheldon. Mater. Today. 7, 44-49 (2004).

[32] S. Peng, K. Cho, P. Qi, H. Dai. Chem. Phys. Lett. 387, 271-276 (2004).

[33] T.A. Saleh, V.K. Gupta. ESPR. 19, 1224-1228 (2012).

[34] Y.S. Su, A. Manthiram. J. Chem. Soc., Chem. Commun. 48, 8817-8819 (2012).

[35] E.F. Antunes, A.O. Lobo, E.J. Corat, V.J. Trava-Airoldi, A.A. Martin, C. Veríssimo. Carbon. 44, 2202-2211 (2006).

[36] A.K. Kota, B.H. Cipriano, M.K. Duesterberg, A.L. Gershon, D. Powell, S.R. Raghavan, H.A. Bruck. Macromolecules. 40, 7400-7406 (2007).

[37] S. Hong, S. Myung. Nat. Nanotechnol. 2, 207–208 (2007).

[38] J.O. Aguilar, J.R. Bautista-Quijano, F. Avilés. Express Polym. Lett. 4, 292-299 (2010).

[39] M.L. Yola, T. Eren, N. Atar. Biosens. Bioelectron. 60, 277-285 (2014).

[40] F. Khaleghi, Z. Arab, V.K. Gupta, M. R. Ganjali, P.N. Atar, M.L. Yola. J. Mol. Liq. 221, 666-672 (2016).

[41] J.A. Fishel, V.J. Santos, G.E. Loeb. In 2008 2nd IEEE RAS & EMBS International Conference on Biomedical Robotics and Biomechatronics. IEEE, 659-663 (2008).

[42] C. Wei, L. Dai, A. Roy, T.B. Tolle. J. Am. Chem. Soc. 128, 1412-1413 (2006).

[43] M.L. Yola, N. Atar. Electrochim. Acta. 119, 24-31 (2014).

[44] K.M. Hassan, T.J. Fahimeh, N. Atar, M.L. Yola, V.K. Gupta, A.A. Ensafi. Ind. Eng. Chem. Res. 54, 3634-3639 (2015).

[45] B. Ertan, T. Eren, İ. Ermiş, H. Saral, N. Atar, M.L. Yola. J. Colloid Interface Sci. 470, 14-21 (2016).

[46] M. Park, H. Kim, J.P. Youngblood. Nanotechnology. 19, 055705 (2008).

[47] M.H. Al-Saleh, U. Sundararaj. Carbon. 47, 1738-1746 (2009).

[48] Michel S, Zhang XQ, Wissler M, Löwe C and Kovacs G, Polym Int 59: 391-399 (2010).
[49] Yang Y, Gupta MC, Dudley KL and Lawrence RW, Adv. Mater. 17: 1999-2003 (2005).
[50] Shafieizadegan - Esfahani AR, Katbab AA, Pakdaman AR, Dehkhoda P, Shams MH and Ghorbani A, Polym. Compos. 33: 397-403 (2012).
[51] Kanaun S and Kochekseraii SB, Int. J. Eng. Sci. 50: 124-131 (2012).
[52] Klicker KA, Schulze WA and Biggers JV, J. Am. Ceram. Soc. 65: C208-C210 (1982).
[53] Xu XB, Li ZM, Shi L, Bian XC and Xiang ZD, Small 3: 408-411 (2007).
[54] C. Guo, Y. Kondo, C. Takai, M. Fuji. Journal of Materials Science: Materials in Electronics, 1-10 (2017).
[55] W.J. Kim, M. Taya, M.N. Nguyen. Mech. Mater. 41, 1116-1124 (2009).
[56] G.D. Seidel, D.C. Lagoudas. J. Compos. Mater. 43, 917-941 (2009).
[57] F. Carmona, R. Canet, P. Delhaes. J. Appl. Phys. 61, 2550-2557 (1987).
[58] M. Taya, W.J. Kim, K. Ono. Mech. Mater. 28, 53-59 (1998).
[59] F. Deng, Q. Zheng. Appl. Phys. Lett. 92, 071902 (2008).
[60] X. Zhang, Y. Pan, Q. Zheng, X. Yi. J Polym Sci B Polym Phys. 38, 2739-2749 (2000).
[61] X.W. Zhang, Y. Pan, Q. Zheng, X.S. Yi. Polym. Int. 50, 229-236 (2001).
[62] C. Guo, Y. Kondo, C. Takai, M. Fuji. Polym. Int. (2016).
[63] Byrne MT, Gun'ko YK, Adv. Mater. 22: 1672-1688 (2010).
[64] Hao X, Gai G, Yang Y, Zhang Y and Nan CW, Mater. Chem. Phys. 109: 15-19 (2008).
[65] Finegan IC and Tibbetts GG, J. Mater. Res. 16: 1668-1674 (2001).
[66] Zhang C, Wang L, Wang J and Ma CA, Carbon 46: 2053-2058 (2008).
[67] Taya M, Kim WJ and Ono K, Mech. Mater. 28: 53-59 (1998).
[68] Li C, Thostenson ET and Chou TW, Appl. Phys. Lett. 91: 223114 (2007).
[69] Li J, Ma PC, Chow WS, To CK, Tang BZ and Kim JK, Adv. Funct. Mater. 17: 3207-3215 (2007).
[70] Seidel GD and Lagoudas DC, J. Compos. Mater. 43: 917-941 (2009).